ELSEVIER

J. Non-Newtonian Fluid Mech. 98 (2001) 185–199

Journal of Non-Newtonian Fluid Mechanics

www.elsevier.com/locate/jnnfm

The effect of channel geometry and wall boundary conditions on the formation of extrusion surface instabilities for LLDPE

Rulande P.G. Rutgers [a,*], Malcolm R. Mackley [b]

[a] *Department of Chemical Engineering, University of Queensland, Brisbane 4072, Qld, Australia*
[b] *Department of Chemical Engineering, University of Cambridge, Pembroke Street, Cambridge CB2 3RA, UK*

Received 20 October 2000; received in revised form 24 January 2001

Abstract

It is believed that surface instabilities can occur during the extrusion of linear low density polyethylene due to high extensional stresses at the exit of the die. Local crack development can occur at a critical stress level when melt rupture is reached. This high extensional stress results from the rearrangement of the flow at the boundary transition between the wall exit and the free surface. The stress is highest at the extrudate surface and decreases into the bulk of the material. The location of the region where the critical level is reached can determine the amplitude of the extrudate surface distortion. This paper studies the effect of wall slip on the numerically simulated extensional stress level at the die exit and correlates this to the experimentally determined amplitude of the surface instability. The effect of die exit radius and die wall roughness on extrusion surface instabilities is also correlated to the exit stress level in the same way. Whereas full slip may completely suppress the surface instability, a reduction in the exit stress level and instability amplitude is also shown for a rounded die exit and a slight increase in instability is shown to result from a rough die wall. A surface instability map demonstrates how the shear rate for onset of extrusion surface instabilities can be predicted on the basis of melt strength measurements and simulated stress peaks at the exit of the die.

Keywords: Surface instabilities; Linear low density polyethylene; Wall slip; Die design

1. Introduction

Surface instability phenomenon that can occur during the extrusion of polyethylene melt has, in the past, been thoroughly researched. In particular, a surface instability, which plays a limiting role on the film blowing rate of linear low density polyethylene (LLDPE) has been reviewed by [1,2]. One of the most favoured mechanisms to explain the onset and development of this instability was first proposed by Cogswell [3] and involves local melt rupture of the extrudate surface at the exit of the die. No universal

* Corresponding author. Fax: +61-7-3365-4199.
E-mail address: rulander@cheque.uq.edu.au (R.P.G. Rutgers).

0377-0257/01/$ – see front matter
PII: S0377-0257(01)00103-3

agreement has as yet been reached on this mechanism (see for example [4–8]), and the authors of this paper provide a summarised overview of other mechanisms proposed for this instability elsewhere [9]. The present work aims to provide further evidence for the validity of the Cogswell concept and also demonstrate the potential to predict the extent of the surface instability as a function of material rheology, melt strength and flow conditions.

A peak in the extensional stress level is reached at the extrudate surface at the exit of the die, because of the rearrangement of the flow field due to the transition from no-slip at the die wall to a free surface boundary condition. This extensional stress level may reach critical values for melt rupture dependent on material properties such as melt elasticity. This critical level is defined by melt strength measurements in uniaxial extension [9]. The Cogswell model conjectures that local cracks appear in the extrudate and temporarily relieves the stress. Much experimental evidence to support this mechanism was provided by [10]. The correlation between the instability wavelength and numerical simulations of the extensional stress region were recently carried out by [11], and the quantitative correlation between the magnitude of the extensional stress at the die exit and the amplitude of the instability was researched in this laboratory [9,12,13].

The present work studies the effect of the modification to the die exit geometry and wall structure on the extrusion surface instability and aims to correlate the amplitude of the instability to extensional stress levels for the various dies.

1.1. The effect of die geometry

Dependence of extrusion surface instabilities on die geometry parameters such as entry angle, length and diameter or gap width was investigated amongst others by [9,11,14,15]. It has been clearly demonstrated that the instability scales linearly with die diameter [15] and it is generally accepted that it is independent of die length [11] and entry angle. The effect of die exit geometry is not reported; all documented studies deal with sharp die exits.

1.2. The effect of die wall roughness

Die wall roughness has only received a very limited attention as a relevant factor in surface instabilities. Scratching with abrasive paper of a PTFE capillary die in the direction of the flow or at right angles to the flow was shown to produce the respective effects of reducing and increasing the severity of surface instability [10].

1.3. The influence of die wall material

The effect of various die wall materials has been investigated by [16–19]. In addition to the well-documented elimination of surface instabilities in PTFE dies through wall slip (see e.g. [10]), recent findings by [19] confirm that apparent wall slip along the slit also explains the absence of surface instabilities when extruding through die materials such as oxide-free brass. Whether this wall slip involves a cohesive or adhesive failure is not as yet resolved.

It is likely but not wholly confirmed that the differences observed for the whole range of die wall materials studied in the early work by [16] can be explained by the extent of slip at the wall. This early work showed that the critical stress for onset of loss-of-gloss of the extrudate ranges as follows: beryllium

copper < copper < aluminium < carbon steel < bronze < stainless steel < α-brass. But later repeats of these experiments on some of the materials [18], [5] showed that the extent of surface instability was dependent on the level of surface oxidation, and could be explained through difference in slip behaviour.

1.4. The effect of wall slip

In an attempt to delay instabilities and to prove the role of boundary conditions, coating of the die wall with materials of low surface energy (generally polytetrafluoroethylene (PTFE)) has been extensively researched (e.g. [5,10,14,15]). Alternatively, fluorocarbon additives have been used in the melt (see for example [17,20]). The combined observations of reduced die swell, a downward shift of the flow curve (stress versus shear rate), and a delay of surface instabilities indicate that the fluoropolymer causes slip at the wall and relieves the critical conditions necessary for surface instabilities.

The localised application of a low energy surface at the exit has a similar effect in eliminating or delaying instabilities. The most elegant demonstration of this effect was provided by [10] using a PTFE insert on the last 5 mm of one half of the capillary die. This reinforces the belief that the instability originates at the exit.

The elimination or delay of surface instability in the presence of slip can be explained on the basis of the change in the exit boundary discontinuity. Under no slip conditions the surface material significantly accelerates from the no-slip to free surface plug flow, whereas the transition from slipping plug flow to free surface plug flow by definition causes less acceleration, particularly as die swell is now also reduced.

The fact that the fracture mechanism due to extensional stresses has not yet been globally accepted, is partly due to the fact that "no reliable results exist for viscoelastic fluids" [4] for the magnitude of the extensional stresses involved. The numerically simulated extensional stress peaks during surface instability have been successfully correlated to Rheotens melt rupture stresses in a companion paper [9] for various flow conditions and die geometries.

The present work demonstrates that the change in the extensional stresses can account for the differences observed between PTFE and stainless steel dies. Furthermore, the effect of the die exit radius and the die wall roughness is also shown to be due to changes in the extensional stresses as compared to a smooth stainless steel die.

2. Materials and methods

2.1. Polymers and die geometries studied

The materials studied were two C6 LLDPE grades, LL09 and LL05, supplied by BP Chemicals (now BP), with melt flow indices (MI) of 0.9 and 0.5, respectively. The molecular masses determined from GPC measurements were $M_w = 118 \times 10^3$ and $M_w = 140 \times 10^3$, respectively, with comparable molecular mass distributions (MMD) of order $M_w/M_n = 4$ (4.23 and 3.93, respectively). The rheological behaviour of the materials was modelled using a KBKZ integral constitutive equation with a Wagner type irreversible damping factor [21,22]. This method of rheological characterisation is described in [23]. The relaxation spectrum covers relaxation times of 10^{-3} to 10^2 s. The spectra and damping factors obtained in simple shear are given in Table 1. LL05, the lower MI material with the slightly higher molar mass and narrower MWD, exhibits significantly higher elasticity than LL09.

Table 1
Rheological parameters of the melts

λ_i (s)	LL09 (g_i (Pa))	LL05 (g_i (Pa))
2.00×10^{-3}	1.56×10^{5}	2.30×10^{5}
9.38×10^{-3}	1.70×10^{5}	2.48×10^{5}
4.40×10^{-2}	5.40×10^{4}	9.89×10^{4}
2.06×10^{-1}	1.92×10^{4}	3.71×10^{4}
9.69×10^{-1}	3.73×10^{3}	8.61×10^{3}
4.54×10^{0}	6.86×10^{2}	1.60×10^{3}
2.13×10^{1}	1.55×10^{2}	2.74×10^{2}
1.00×10^{2}	3.39×10^{1}	9.11×10^{1}
k (–)	0.24	0.25

The flow studied is an abrupt (180°) contraction planar flow with a free surface die swell. The conditions and equipment for extrusion and flow visualisation were discussed previously [12]. The die geometries studied were manufactured by Cambridge Reactor Design and are given in Table 2. Here, w: gap width, d: depth, L: length, and W/w: contraction ratio. The stainless steel dies were polished to an average roughness of approximately $R_a = 1$ μm apart from those with saw tooth profiles of 0.1 and 0.5 mm depth in the direction of the flow. The die inserts with a solid PTFE layer on the last 7 out of the 8 mm long slit wall are shown in Fig. 1.

Experimental global stress fields where obtained through optical birefringence measurements, using the experimentally determined stress optical coefficient of $2.03 \pm 0.11 \times 10^{-9}$ Pa^{-1} at 180°C [13].

2.2. Die and extrudate surface characterisation

The extrudate surface was investigated with scanning electron microscopy (SEM), and the observed semi-periodic wave-like distortion was quantified using a number of Taylor Hobson stylus surface profile measurement instruments (Form Talisurf+ and Form Talysurf 120-L).

The extrudate roughness in the direction of the flow is expressed in terms of the tribological parameter R_{zDIN} as a measure of amplitude. R_{zDIN} is the average height difference between the five highest peaks and the five lowest valleys in the sampling length, subsequently averaged over the total assessment length (five times the sampling length). The sampling length is a user-defined cut-off length, which filters out any waviness in the extrudate.

Table 2
Die dimensions, material and surface finish (average roughness R_a)

Die	w (mm)	L (mm)	d (mm)	W/w (–)	Material	R_a (mm)
1	1.125	8.03	15.00	13.3	Steel	0.5
2	1.125	8.01	15.01	13.3	Steel	25
3	1.160	7.51	15.01	12.9	Steel	125
4	1.125	7.50[a]	15.00	13.3	Steel	–
5	1.125	8.01	15.01	13.3	PTFE	–

[a] Exit with 0.5 mm radius.

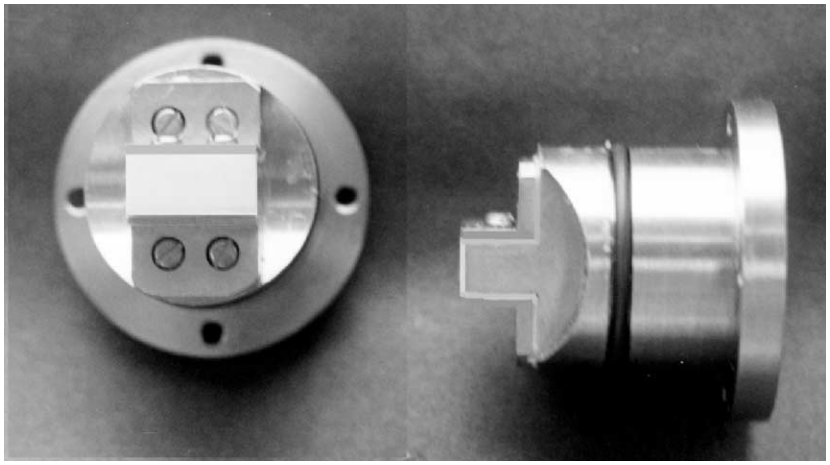

Fig. 1. Die inserts with solid PTFE layer.

Routine calibrations and 3–5 repeat measurements on different locations of each sample were carried out to obtain the presented results. The non-destructive effect of the stylus on the extrudate and the applicability of the measurement technique given the stylus tip dimensions was verified. This same method was used to characterise the surface finish of the die inserts: Fig. 2 shows the relative roughness of the smooth stainless steel die and both saw tooth die walls. It is clear that compared to polymer chain length scales even the smooth die wall cannot be considered as a flat plane.

2.3. Numerical simulation of the flow

The commercial package Polyflow was used for the numerical simulation of the steady flow. The boundary conditions used for the simulation were fully developed flow 25 mm upstream from the slit entrance, zero slip velocity at the wall for all except the PTFE die; symmetry along the centre plane; and

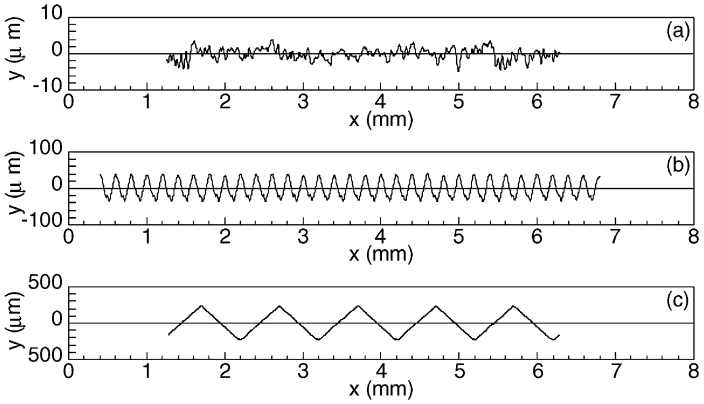

Fig. 2. Surface roughness of die inserts: profiles measured in direction parallel to the flow. (a) Smooth die 1 (die wall roughness $R_a = 1.25\ \mu m$); (b) die 2 with 0.1 μm saw tooth profile ($R_a = 25\ \mu m$); (c) die 3 with 0.5 μm saw tooth profile ($R_a = 125\ \mu m$).

a 80 mm long free surface with zero force at the outlet. The validation of the numerical simulation against experimental pressure difference, end pressure losses, die swell, centreline velocities and centreline principal stress difference (PSD) profiles obtained from stress birefringence measurements has been described previously [12]. The match of the numerical simulation with experimental data was relatively good and lie within the estimated experimental and numerical error of 9 and 12%, respectively [13], although the elongational behaviour of LL05 is less well predicted than that of LL09.

The flow region of particular interest for this study is the die exit. Based on a mesh sensitivity analysis [9] a mesh of 425 elements with quadratic interpolation for velocities, linear interpolation for pressure and local refinement near the entry and exit singularities was used to simulate the flow behaviour in the standard stainless steel die (die nr. 1, see Table 1). It was shown previously [9] that reasonably accurate predictions of the flow behaviour could be obtained when investigating the flow along the streamlines at distances down to 50 μm from the wall. The simulation was shown to converge to the same solution for all meshes, except in the element immediately adjacent to the exit singularity, where the predicted stress increases with reduced element size. This highly localised numerical artefact does not cause a mesh dependence of the simulated exit stress peak outside the one element. The element sizes at the die exit of the meshes investigated were 4 μm × 4 μm, 8 μm × 8 μm and 16 μm × 16 μm, respectively, which justifies the study of the streamline at 50 μm from the wall as a conservative indication of the stress and deformation fields to which the surface of the extrudate was submitted. It was demonstrated [9] that if a certain stress level is reached at the die exit at 50 μm from the wall, the stress level closer to the wall under those particular flow conditions is higher, and that the stress level observed at 50 μm from the wall would have been reached under less demanding flow conditions (e.g. lower shear rate or higher temperature) by the melt flowing closer to the wall.

Fig. 3 shows the meshes used for the dies with saw tooth wall profiles (die nr. 2 and 3) and for the die with a rounded exit corner (die nr. 4). Convergence was reached for the 0.5 mm saw tooth die wall with great difficulty, using a Gauss integration rule instead of the Laguerre integration rule used for all other

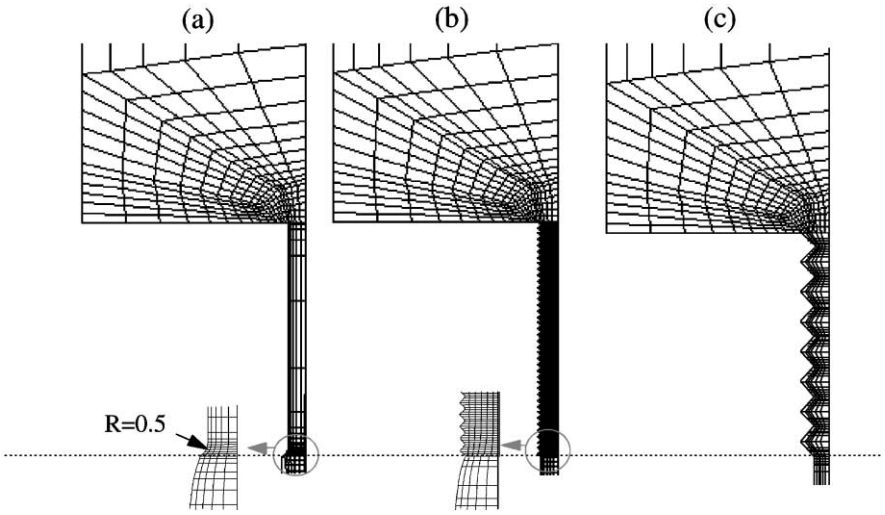

Fig. 3. Meshes for the simulation of various slit die geometries: (a) die 4 with 0.5 mm exit radius; (b) die 2 with 0.1 mm saw tooth roughness; (c) die 3 with 0.5 mm saw tooth roughness.

simulations. This, and a particularly low criterion for zero velocity allows the simulation to converge despite the presence of closed loops due to the many near-stagnant regions in the corners of the teeth. Low flow rates may not be solved due to this problem. For the smaller saw tooth wall, the program failed to reach convergence. The comparison of the global experimental birefringence and the numerically simulated PSD field of LL05 in the 0.5 mm saw tooth die (die nr. 3) is given in Fig. 4. The stress levels, dead zones and stress concentrations are predicted with reasonable accuracy.

The PTFE insert was simulated by replacing the zero tangential velocity for the last 7 mm of the wall by a slip law, commonly given in the form:

$$v_s = a f_s^m, \tag{1}$$

giving the slip velocity v_s as a function of the friction at the wall f_s. In Polyflow this equation is given in the form:

$$f_s = f_{slip} v_s^{ex_{slip}+1}. \tag{2}$$

Thus, the coefficients in the two forms of the slip law are related as follows:

$$f_{slip} = \left(\frac{1}{a}\right)^{1/m}, \tag{3}$$

$$ex_{slip} = \frac{1}{m} - 1. \tag{4}$$

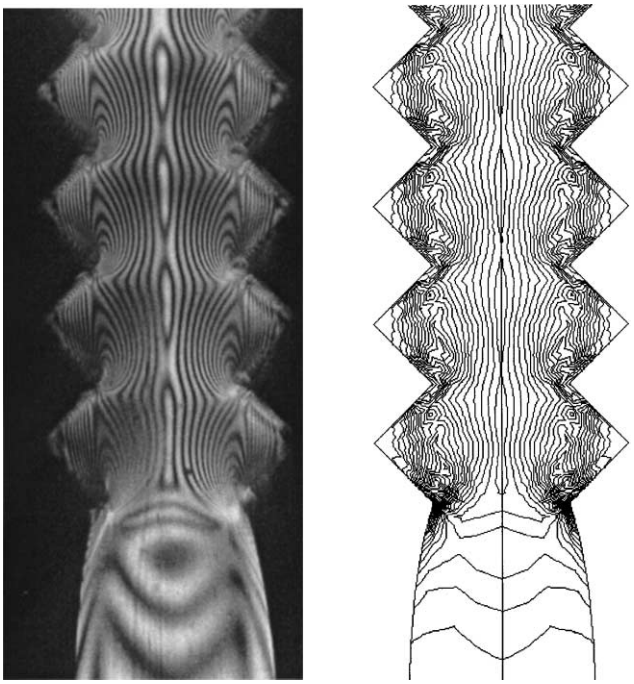

Fig. 4. Exit detail of experimental flow birefringence and numerical simulation of LL05 at 180°C and $\dot{\gamma}_a = 13\,s^{-1}\,m^3/s$ in stainless steel die 3 with 0.5 mm saw tooth profile.

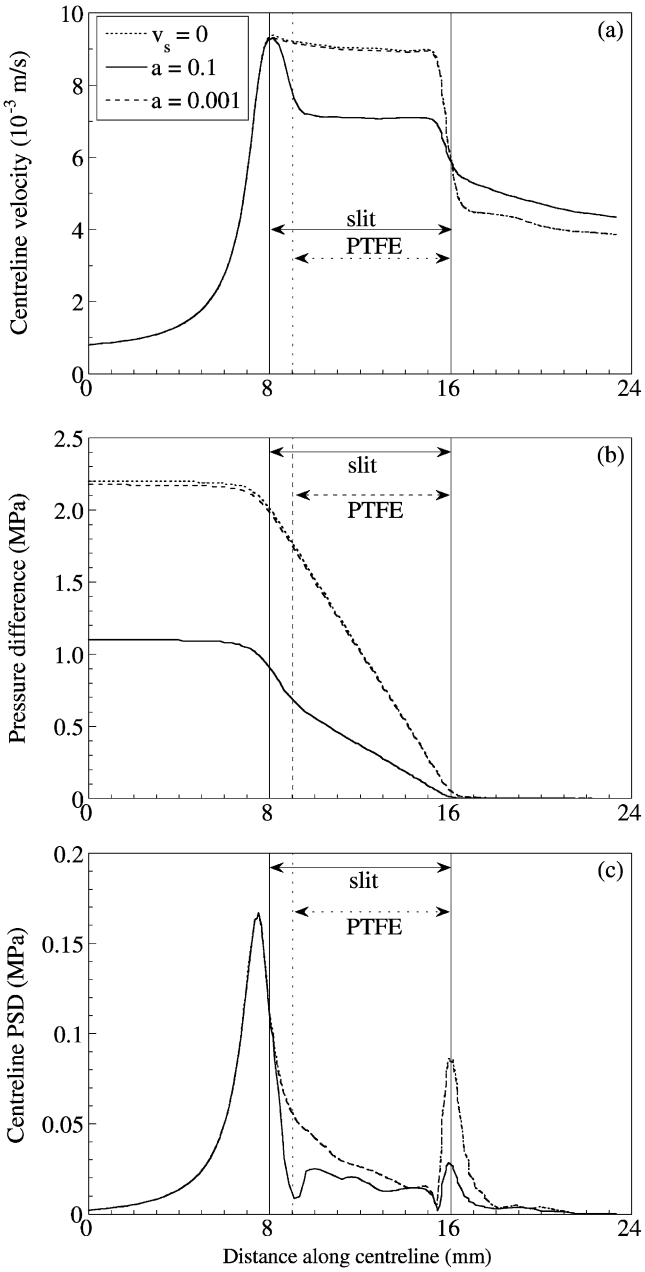

Fig. 5. Flow variables as a function of no slip (dashed line) or slip (continuous line) boundary condition for LL09: (a) centreline velocity profile; (b) pressure difference; (c) centreline PSD profile.

For various non linear slip laws proposed by Hatzikiriakis and Dealy [24] and Person and Denn [18] for polyethylene on stainless steel values of f_{slip} ranging from 6×10^4 to 2×10^5 Pa (s/mm)$^{1/m}$ were found. Therefore, it was estimated that in a linear slip law approximation (i.e. $m = 1$) f_{slip} values of 10^6 and 10^4 Pa s/mm would represent non-slip steel and slippery PTFE, respectively, corresponding to slip coefficients $a = 0.001$ and $a = 0.1$, respectively. Using this condition to simulate zero slip on steel should give comparable results to the boundary condition of zero slip velocity, whereas the PTFE slip condition should result in approximately 20% experimental reduction in pressure drop. It must be noted that due to the experimental difficulty in maintaining a stable PTFE insert, little reliable experimental data was available and therefore the slip law assumed here is considered a rough approximation. The predicted flow conditions plotted as a function of the various slip and no slip boundary conditions are given in Fig. 5 ((a) centreline velocity; (b) pressure difference and (c) centreline PSD). The graphs show that the two variants of no slip boundary condition give comparable results and that the slip boundary condition overestimates the reduction in pressure difference along the slit. It is furthermore observed that the entry stress peak is not affected by the no slip condition but that the exit stress is significantly reduced, due to the reduction in extensional flow resulting from the transition from slip to free plug flow of the extrudate as compared to the transition from a no-slip near-parabolic velocity profile to free plug flow. Fig. 6 gives the global PSD isoclines, which clearly shows the reduction of stress concentrations at the die exit and extrudate surface as well as a reduction in die swell. Stress concentration is visible at the transition from no-slip to slip condition but the overall stress level in the die land is significantly reduced.

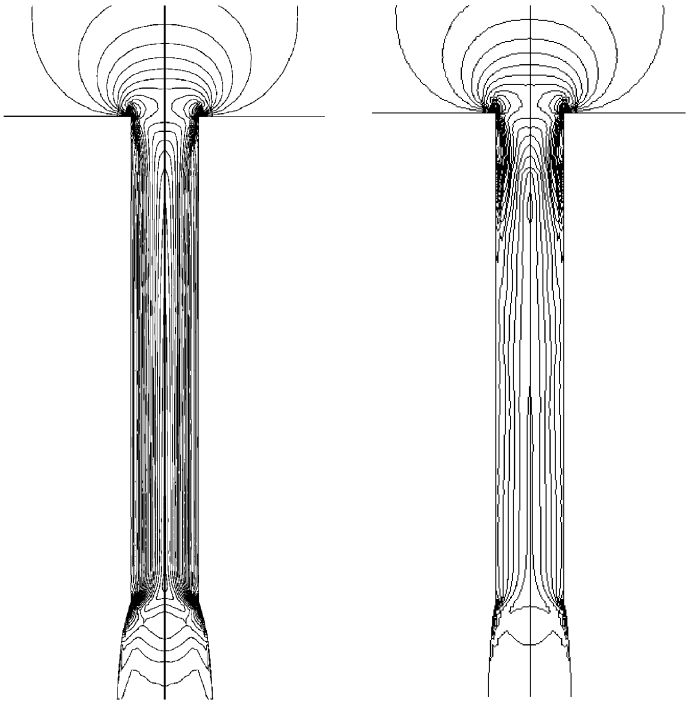

Fig. 6. Predicted global stress field of LL09 at 180°C and $\dot{\gamma}_a = 35\,s^{-1}$ for (a) stainless steel die 1 with zero slip velocity at the wall and (b) PTFE die 5 with slip coefficient $a = 0.1$.

2.4. Rheotens measurements of melt rupture stress

The measurement of critical stress for melt failure may be determined through Rheotens measurements. The experimental set-up and procedure of Rheotens rupture measurements is described by [9,25]. In this manner critical stress levels may be obtained for each material at selected temperatures. The critical stress level for rupture of LL09 and LL05 is of order 0.8–1 MPa and shows a slight dependence on the shear rate in the upstream capillary.

3. Results and discussion

3.1. Experimental study of the onset and growth of the instability

3.1.1. Dependence on exit geometry and wall material

The amplitude of the surface instability for LLDPE flow through a stainless steel die is shown in Fig. 7 to increase with apparent wall shear rate and to reach levels of order 100 μm. Fig. 7 demonstrates that this effect is substantially reduced in the presence of a rounded die exit and effectively eliminated in the presence of a PTFE wall. These results suggest that a round exit reduces the severity of the flow transition of the material exiting from the die at the surface of the extrudate and that the stresses generated at the exit of the PTFE die is reduced to well below critical levels. It is suggested that the material slips significantly along the PTFE wall and that therefore the change in velocity of the surface material is much smaller than in a stainless steel die, resulting in a significant reduction in stress.

3.1.2. Dependence on wall roughness

Fig. 8 shows the amplitude of the extrudate surface instability as a function of shear rate for the three dies with different surface finish: $R_a = 0.5\,\mu m$; $R_a = 25\,\mu m$ and $R_a = 125\,\mu m$, respectively. It appears that the instability develops at a lower shear rate in the 25 μm saw tooth die, whereas the effect is insignificant for the larger scale saw tooth die wall. It is noted however, that for the 25 μm saw tooth die the instability amplitude is only observed to be significantly larger at one shear rate, $35\,s^{-1}$, and that

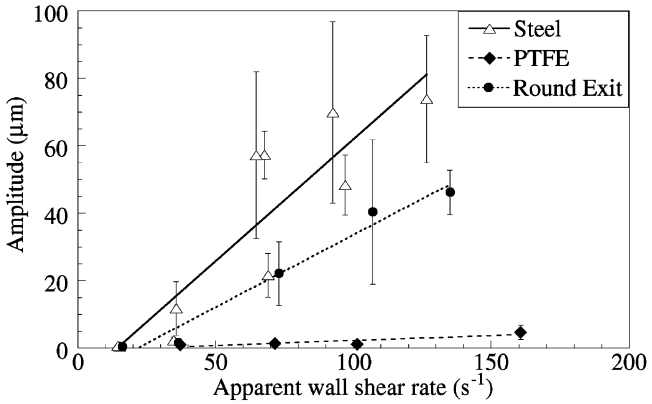

Fig. 7. Amplitude of surface roughness of LL05 extruded at 180°C as a function of die wall and exit design. Open triangles: smooth stainless steel die 1; diamonds: PTFE die 5; circles: stainless steel die 4 with rounded exit lip.

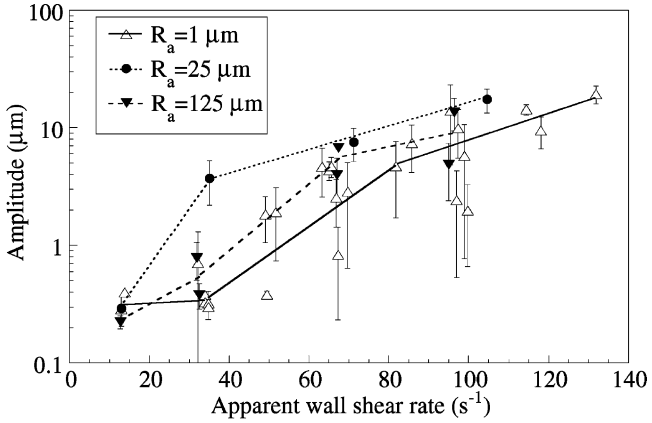

Fig. 8. Amplitude of surface roughness of LL09 extruded at 180°C as a function of die wall roughness. Open triangles: smooth wall ($R_a = 1$ μm); closed circles: small saw tooth ridges ($R_a = 25$ μm); closed triangles: large saw tooth ridges ($R_a = 125$ μm).

therefore it is impossible to make conclusive statements on the effect of the small scale wall roughness. It is conceivable that the history of the material flowing close to a rough wall were altered such as to intensify the stress condition at the exit of the die. For the 125 μm saw tooth die, however it appears that the scale of the saw tooth is too macroscopic to have any effect on the condition of the material at the die exit.

3.2. Correlation between predicted local stress conditions and the onset of instabilities

3.2.1. Numerical study of flow conditions near the die exit

The simulated principal stress difference along the streamline at 50 μm from the wall is shown for a smooth stainless steel die and a PTFE die in Fig. 9. The stress first reduces on compression in the entrant corner of the die and subsequently increases to a small peak at the entry of the die. Whereas the stress in the stainless steel die remains constant along the die land, it reduces significantly in the PTFE die upon

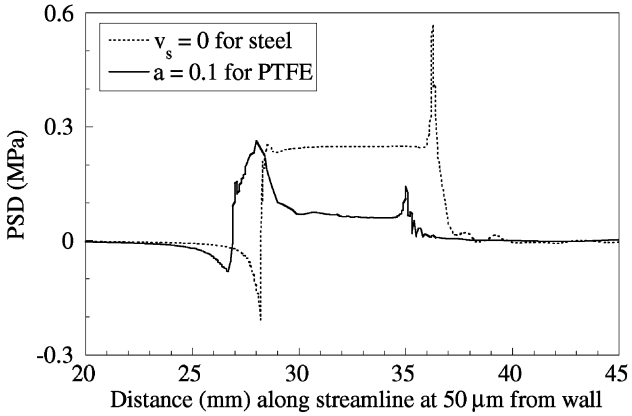

Fig. 9. Simulated PSD along the streamline at 50 μm from the wall for LL09 extrusion through a stainless steel die with zero slip at the wall (continuous line) and a PTFE die with a slip coefficient of 0.1 (dashed line).

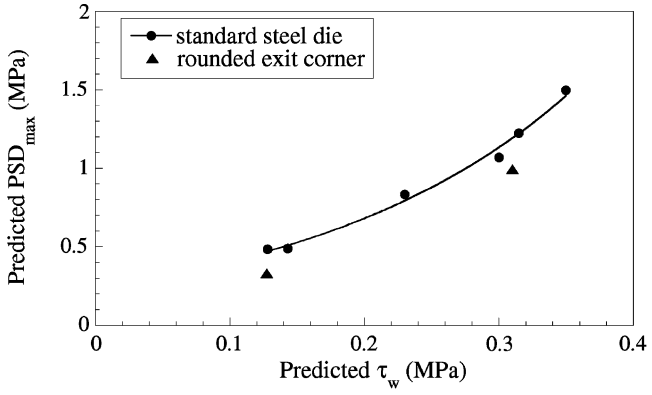

Fig. 10. The effect of die wall roughness and slip: simulated PSD exit peak for LL09 at 180°C extruded from stainless steel die 1 with smooth surface finish (squares); stainless steel die 3 with 0.5 mm saw teeth (triangles) and PTFE die 5 (circles).

the transition to the slip boundary condition. At the die exit a large peak occurs due to the acceleration from a zero slip boundary condition to free flow. This peak is significantly reduced in the case of the simulated PTFE die where the transition is from a slip condition to free flow. In the case of the PTFE die the stress at the exit is lower than the stress at the die entry.

The magnitude of the PSD exit peak is shown as a function of shear rate in Fig. 10. The exit stress peak increases with shear stress as does the amplitude of the instability and the stress decreases with a rounded die exit as does the instability amplitude.

Fig. 11 shows the effect of the large scale saw tooth die wall roughness on the simulated exit PSD peak, which is slightly increased. The shear rate is obviously not constant along the macroscopically rough die wall, therefore, the shear rate is taken at the extremity of the saw tooth where the die gap is the same as that of the smooth die and which is the shear rate at the exit of the die. This oscillation in shear rate along the streamline introduces a level of uncertainty in the shear rate. We therefore suggest that the significance of the effect of the saw tooth die wall roughness on the exit stress peak is not conclusive. It is however suggested that the stress experienced by the material in either of the two rough dies may

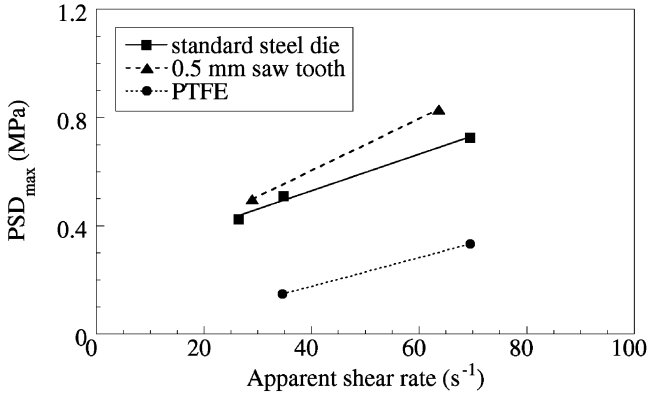

Fig. 11. Simulated PSD exit peak for LL05 at 180°C in die 1 with sharp exit radius (circles) and die 4 with a rounded exit radius (triangles).

be larger than that in the smooth die as it experiences an accumulation of several effects at the same point: (a) acceleration to free flow; (b) acceleration from a slightly wider die gap to a narrower die gap; (c) a maximum in the shear rate. The latter two effects are periodic effects along the die land, which may furthermore influence the memory of the deformation history of the material. The flow birefringence pattern and the flow simulations reported here for the 125 μm rough die wall show however, that the stress patterns are identical at each saw tooth along the die land (Fig. 4). This may not necessarily be the case for the smaller scale saw tooth. A more severe extrusion surface instability in the 25 μm rough die could thus be assigned to an increase in exit stress. However, the limited experimental evidence and the lack of convergence for this geometry do not allow us to make conclusive statements to this effect.

3.2.2. Instability map

The above discussion demonstrates a correlation between the amplitude of the extrusion surface instability and the magnitude of the peak in principal stress difference at the exit of the die. It is therefore suggested that the onset of the instability is related to a critical extensional stress beyond which local rupture of the melt occurs. It was shown that the extensional stress was highest at the surface at the exit of the die and therefore it is clear that a critical stress level would first be reached at the surface and only at more severe conditions (e.g. higher flow rate) at distances further from the surface. Small amplitude cracks occur at low shear rates when the critical stress is reached at the surface, larger amplitude cracks may occur if the critical stress is reached further into the surface, allowing cracks to grow until a region is reached where the stress is so low that crack growth is no longer energetically viable. This mechanism could explain the increase in the amplitude of the instability with an increasing peak of PSD at the die exit. The critical stress level required for melt rupture may be obtained from the stress at rupture in Rheotens measurements and is found to be of order 0.8–1 MPa [9].

Fig. 12 represents an instability map which summarises the results reported in this paper and compares the exit stress peaks in the various dies to the Rheotens melt rupture stress. It furthermore relates the level

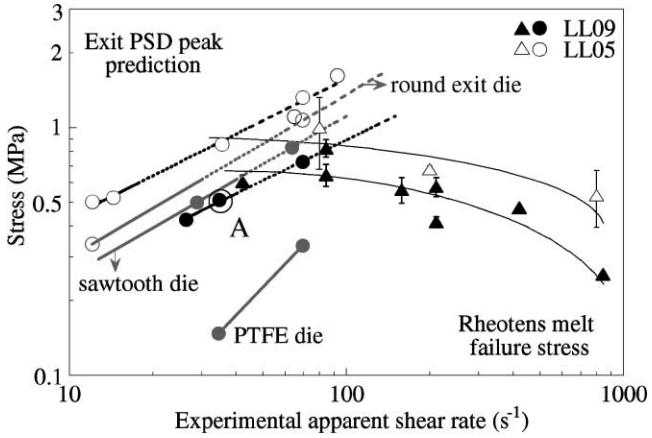

Fig. 12. Surface instability map for LL09 (closed symbols) and LL05 (open symbols). Circles indicate the simulated peak values of PSD at the die exit, triangles indicate the Rheotens rupture stress. The lines linking the PSD data indicate the level of surface extrudate roughness: continuous: smooth extrudate; dotted: extrudate roughness 1–10 μm; dashed instability amplitude 10–100 μm. $T = 180^{\circ}$C. Black data obtained in die 1, grey data obtained in die 3 (125 μm saw tooth), die 4 (round-exit) and die 5 (PTFE) as indicated.

of the stress peak to the amplitude of the extrusion instability. A continuous line indicates no instability, a dotted line indicates extrudate roughness of 1–10 μm, and a dashed line indicates instability of 10–100 μm amplitude. For example at data point A, LL09 flows through a stainless steel smooth die at a wall shear rate of 35 s^{-1}. Under these conditions the extrudate is smooth, indicated by a continuous black line, and the simulated exit stress peak is 0.5 MPa. As the shear rate is increased the extrudate becomes rough (dotted line) and the instability develops fully (dashed line) as the exit stress level reaches the level of 1 MPa (along the streamline 50 μm from the surface). The Rheotens melt rupture stress for this material at this shear rate is of order 0.75 MPa. The extrudate distortion is of order 10 μm in amplitude when this critical stress is reached at the exit. The surface distortion is measured on the cooled extrudate, hence some relaxation of the distortion will have reduced the original amplitude of the effect. Without attaching too much significance to the quantitative precision of the values of the simulated exit stress peaks, it is clear that instabilities occur as exit stress levels are reached which are the same order of magnitude as the critical stress for melt rupture. The observed trends in surface instability for the two grades of LLDPE and for the different dies with a rounded die exit, a saw tooth roughness or in particular a PTFE surface, can all be explained in terms of the extensional stress peak level as shown in Fig. 12. The extrudate is smooth for all cases where the extensional stress peak is below 0.5 MPa. Above this value, small scale instabilities are observed which reach an amplitude of 10–100 μm as the exit stress level reaches the critical value for melt rupture of 1 MPa.

4. Conclusions

This work demonstrates a correlation between the amplitude of extrusion surface instability and the numerically simulated peak in extensional stress at the exit of the die for LLDPE extrusion. It was shown that when a critical stress level of order 0.8–1 MPa is reached in the material at the extrudate surface at the exit of the die, extrusion surface instability is observed with an amplitude of order 100 μm. It is this critical extensional stress level rather than shear rate or shear stress that appears to controls the onset and severity of the extrusion instability, and this correlation holds true across two LLDPE grades, various die wall structures and a modified die exit geometry. This work reconfirms the role of the extensional stress peak at the die exit previously shown [9] to determine the amplitude of extrusion surface instability in various die gaps and lengths.

The correlation of the critical extensional stress level observed for the instability and the critical stress level using a Rheotens melt rupture measurements suggests that a melt rupture mechanism is operational, which results in small local crack formation of the extrudate at the exit of the die. The extent to which the cracks travel inwards into the bulk of the die is suggested to be directly related to the distance from the surface at which the extensional stress level is lower than the critical level for crack propagation. Exactly to what extent this level is lower than the level required for crack initiation in polymer melts requires further investigation and in addition the presence of the crack itself will also modify local stress conditions thereby increasing the level of complexity.

Acknowledgements

This work was made possible through a CASE award funded by the EPSRC and BP Chemicals (now BP). The authors thank D.G. Gilbert from BP Chemicals for inspiring discussions and A. Goublomme

from Polyflow S.A. for advice. Rheotens experiments and related knowledge were kindly provided by A. Bernnat and M.H. Wagner. The surface profile measurement equipment was made available by Taylor Hobson Pneumo.

References

[1] M.M. Denn, Annu. Rev. Fluid Mech. 22 (1) (1990) 13–34.
[2] R.G. Larson, Rheol. Acta 31 (1992) 213–263.
[3] F.N. Cogswell, J. Non-Newtonian Fluid Mech. 2 (1977) 37–47.
[4] J.R. Barone, N. Plucktaveesak, S.Q. Wang, J. Rheol. 42 (4) (1998) 813–832.
[5] V.G. Ghanta, B.L. Riise, M.M. Denn, J. Rheol. 43 (2) (1999) 435–442.
[6] J. Watson, F.N. Cogswell, J. Rheol. 43 (1) (1999) 245–247.
[7] J.R. Barone, N. Plucktaveesak, S.Q. Wang, J. Rheol. 43 (1) (1999) 248–251.
[8] J.M. Watson, F.N. Cogswell, J. Rheol. 43 (1) (1999) 252–252.
[9] R.P.G. Rutgers, M.R. Mackley, J. Rheol., in press.
[10] J.-M. Piau, N. El Kissi, F. Toussaint, A. Mezghani, Rheol. Acta 34 (1995) 40–57.
[11] C. Venet, B. Vergnes, J. Rheol. 41 (4) (1997) 873–892.
[12] M.R. Mackley, R.P.G. Rutgers, D.G. Gilbert, J. Non-Newtonian Fluid Mech. 76 (1998) 281–297.
[13] R.P.G. Rutgers, An experimental and numerical study of extrusion surface instabilities for polyethylene melts, Ph.D. Thesis, University of Cambridge, UK, 1998.
[14] R.H. Moynihan, D.G. Baird, R. Ramanathan, J. Non Newtonian Fluid Mech. 36 (1990) 255–263.
[15] S.-Q. Wang, P.A. Drda, Y.-W. Inn, J. Rheol. 40 (5) (1996) 875–898.
[16] A.V. Ramamurthy, in: Proceedings of the Xth International Congress on Rheology, Sydney, 1988.
[17] A. Rudinm, H.P. Schreiber, D. Duchesne, Pol. Plast. Tech. Eng. 29 (3) (1990) 199–234.
[18] T. Personm, M.M. Denn, J. Rheol. 41 (2) (1997) 249–265.
[19] S.S. Varennesm, H.P. Schreiber, J. Adhesion 46 (1) (1994) 3–14.
[20] M.H. Laun, in: Proceedings of the 5th European Rheology Conference, Ljubljana, Slovenia, 6–11 September 1998.
[21] M.H. Wagner, Rheol. Acta 15 (1976) 136–142.
[22] M.H. Wagner, Rheol. Acta 18 (1979) 33–50.
[23] M.R. Mackley, R.P.G. Rutgers, in: A.A. Collyer (Ed.), Rheological Measurement, Chapman & Hall, London, 1999, Chapter 5.
[24] S.G. Hatzikiriakos, J.M. Dealy, Intern. Pol. Proc. 8 (1) (1993) 30–35.
[25] M.H. Wagner, A. Bernnat, V. Schulze, Kautchuk Gummi Kunststoffe 50 (9) (1997) 653–659.